



Process development for improved soft X-ray zone plates

J. Reinspach*, M. Lindblom, O.v. Hofsten, M. Bertilson, H.M. Hertz, A. Holmberg

Biomedical and X-ray Physics, Department of Applied Physics, Royal Inst. of Technology, 10691 Stockholm, Sweden

ARTICLE INFO

Article history:

Received 14 September 2009

Received in revised form 3 November 2009

Accepted 4 November 2009

Available online 10 November 2009

Keywords:

Zone plate

Electroplating

Diffraction efficiency

ABSTRACT

We demonstrate two nanofabrication methods which improve the diffraction efficiency of high-resolution soft X-ray nickel zone plates. First, pulse electroplating is shown to result in uniform diffraction efficiency over the entire zone-plate area. A resulting enhancement of the total efficiency of 20% compared to conventional DC plating was measured. Second, we demonstrate that a high-resolution cold development process can be combined with efficiency-enhancing dry etching into an underlying germanium film. We present 16 nm half-pitch gratings composed of 50 nm nickel on top of 50 nm germanium.

© 2009 Elsevier B.V. All rights reserved.

1. Introduction

Nanofabricated zone plates are used as high-resolution objectives in soft X-ray microscopy, e.g., in the water window (2.3–4.4 nm) [1]. Due to the short wavelength X-ray microscopy has potential to perform very high-resolution imaging. In practice, the achievable resolution is determined by the zone-plate optics rather than the wavelength. Therefore improved fabrication methods for high-resolution zone-plate optics are crucial for the development of soft X-ray microscopy. Furthermore, imaging with increased resolution requires longer exposure times to preserve signal-to-noise ratio and contrast [2]. It is therefore desirable that the zone plate objectives have both high resolving power and high diffraction efficiency.

The resolving power is determined by the width of the outermost zone, dr_N , [3] and typical outermost zone widths are in the range of 20–50 nm [4–6]. The diffraction efficiency is dependent on the optical material and its thickness [7]. For a wavelength of 2.48 nm, which we use in our in-house soft X-ray microscope [8], nickel is the most suited material and the diffraction efficiency is maximized at a nickel thickness of ~ 230 nm. Nickel zone plates are fabricated by electroplating into a structured mold, and the achievable aspect-ratio is typically limited to about 4:1 to 5:1. Thus, for high-resolution zone plates the nickel thickness is typically too low and, consequently, the diffraction efficiency is reduced.

In this paper we present two nanofabrication methods for improving diffraction efficiency of high-resolution soft X-ray nickel zone plates. Pulse electroplating has previously been shown to solve the mass distribution problems of direct current (DC) plating and

produce a uniform nickel height over the entire zone plate [9]. Here we demonstrate that pulse plating produces uniform diffraction efficiency over the entire zone plate area and results in an increased total diffraction efficiency. The second method involves nickel-germanium zone plates. We have previously demonstrated that the diffraction efficiency of nickel zone plates can be significantly increased by fabricating the nickel zone plate on a germanium film and subsequently using it as hardmask for a CHF_3 dry etch into the germanium [10]. Here we show that this process can be extended to high-resolution structures by including cold development.

2. Improved diffraction efficiency by pulse plating

Non-uniform mass distribution is a known issue in electroplating [11]. The distribution is determined by factors such as bath composition, sample geometry, and the overall current density. In nickel zone plate fabrication we observe that the deposition rate decreases with zone plate radius when the electroplating is carried out with a direct current (DC), which results in an only partly filled mold in the outermost parts. We have previously demonstrated that the problem of non-uniform mass distribution can be overcome by using pulse or pulse reverse plating [9]. The thickness profile of the zone plate can be controlled by adjusting the pulse parameters, and thus a uniform nickel thickness can be obtained. Below we quantify the benefit of pulse plating by a measurement of the diffraction efficiencies of zone plates fabricated using pulse and DC plating.

2.1. Fabrication process

To evaluate the efficiency enhancement provided by pulse plating, zone plates were fabricated using identical processing parameters with the exception for the electroplating step, in which

* Corresponding author.

E-mail address: julia.reinspach@biox.kth.se (J. Reinspach).

either DC plating or pulse plating was applied. The nickel zone plates were fabricated using our standard fabrication process [12] according to Fig. 1. Silicon nitride membranes with a thickness of 50 nm were used as substrates. The substrates were first coated with a plating base consisting of 5 nm Cr and 10 nm Ge. Thereafter, a trilayer resist was deposited. This comprised a 120 nm thick plating mold material, ARC XL-20 (Brewer Science), a 5 nm Ti hardmask, and a 25 nm thick electron beam resist, ZEP 7000 (Zeon Chem., L.P.). The Cr, Ge, and Ti layers were deposited by electron beam vapor deposition (Edwards Auto 306, 10^{-6} Torr base pressure). The ARC XL-20 and the ZEP 7000 were spin coated and baked in an oven at 170 °C for 180 and 30 min respectively.

The electron beam resist was patterned with a Raith 150 electron-beam system with a dose of $\sim 80 \mu\text{C}/\text{cm}^2$ at 25 kV. The development was carried out in hexyl acetate for 30 s, followed by a rinse step in isopropyl alcohol and subsequently in pentane. The samples were then dried in a flow of hot air. The pattern was transferred to the Ti layer by 160 s of RIE with BCl_3 (Plasmalab 80+, Oxford Instruments) using the following parameters: 10 sccm gas flow, 15 mTorr pressure, and 80 W sample RF power. The Ti was used as a hardmask for a subsequent O_2 RIE (Plasmalab 80+, Oxford Instruments) into the ARC XL-20 plating mold material. The etch parameters were 5 min etch time, 10 sccm gas flow, 50 W sample RF power, and 3 mTorr pressure. After this, the electroplating was performed in a nickel sulfamate bath (Lectro-Nic 10-03, Enthone Inc.) at a temperature of 52 °C and a pH of 3.25. The DC plating was carried out at a constant current density of approximately $0.1 \text{ A}/\text{cm}^2$. The pulse plating was performed at a pulse current density of $\sim 15 \text{ A}/\text{cm}^2$, a pulse length of 1 ms, and a period of 1 s. These parameters were chosen to optimize the uniformity of deposit. After the electroplating was completed, the Ti hardmask and ARC XL-20 plating mold were removed by repeating the aforementioned RIE steps.

2.2. Efficiency measurements

The diffraction efficiency measurements were carried out at $\lambda = 2.88 \text{ nm}$ in our laboratory laser-plasma-based arrangement [13]. With this setup, the total and local first-order diffraction efficiency can be determined. The fabricated zone plates had an outer-

most zone width of 30 nm and a diameter of 58 μm . The nominal plated nickel height was $\sim 100 \text{ nm}$, and thereby the theoretical diffraction efficiency is about 12%. To ensure comparability between the DC and the pulse-plated zone plate, two zone plates with equivalent pattern quality and center nickel height were selected. The zone height was measured by scanning profilometry (Tencor P15) and the pattern quality was evaluated by scanning electron microscopy (SEM). Fig. 2 shows the height profile and the efficiency as a function of radius of the selected zone plates. The nickel height and the first-order diffraction efficiency of the DC-plated zone plate decrease with radius (Fig. 2a and c), whereas the pulse-plated zone plate exhibits a more uniform profile (Fig. 2b and d). The efficiency in the center part of the zone plate is shaded because it cannot be measured with the used method, due to the presence of the zeroth-order beam.

From the measured data, the total efficiency values were calculated and the substrate absorption was compensated for. The total efficiencies, without substrate absorption, were 5.46% for the DC-plated and 6.52% for the pulse-plated zone plate. This is about half the theoretical value for the given nickel height, which is consistent with previously measured zone plates [13]. The resulting efficiency enhancement between DC and pulse-plated zone plates was $\sim 20\%$, which demonstrates that pulse plating improves the diffraction efficiency significantly.

3. High-resolution nickel-germanium zone plates

Another approach to improve the diffraction efficiency is to combine two optical materials, i.e. nickel and germanium, in one zone plate [10]. Fig. 3a illustrates the fabrication process. A nickel zone plate is first fabricated on a germanium film and then used as hardmask for a dry etch into the underlying germanium. In a proof-of-principle experiment we showed that this method can double the diffraction efficiency for zone plates with $dr_N = 25 \text{ nm}$ [10]. In this section we take the method a step further and show that it is suitable for zone plates with dr_N down to at least 16 nm. This is demonstrated by applying the nickel-germanium concept to 16 nm half-pitch gratings. The key improvement is the use of cold development, which we describe in detail elsewhere [14].

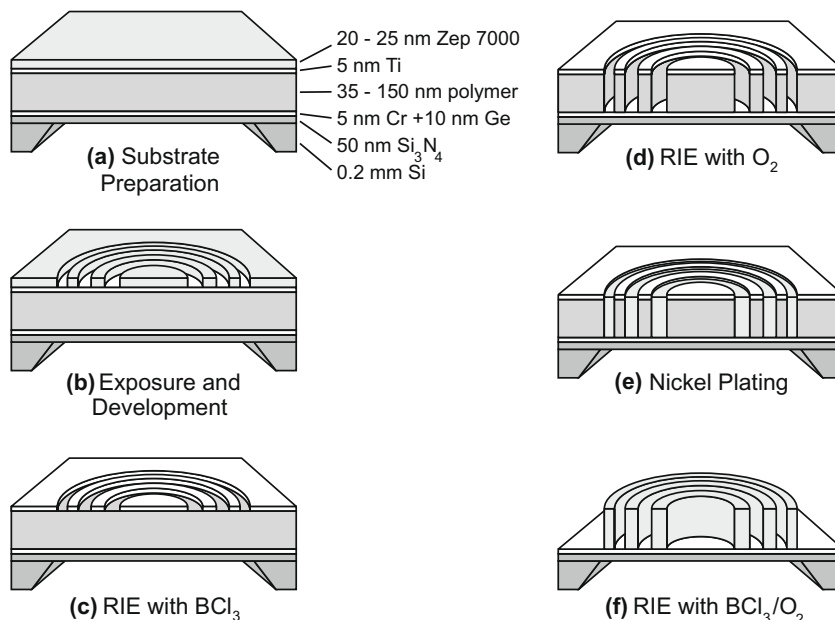


Fig. 1. The standard fabrication process for nickel zone plates.

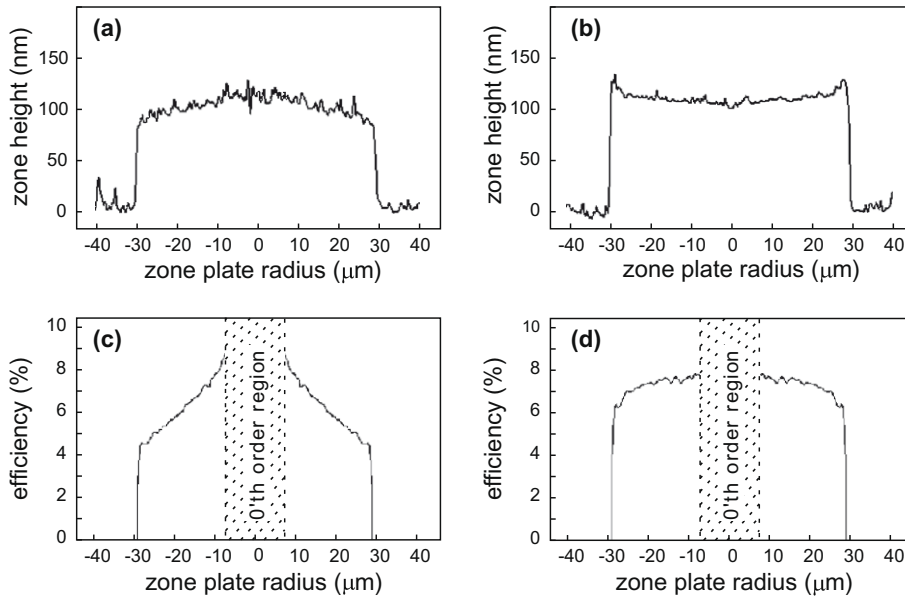


Fig. 2. The nickel profile of a DC-plated zone plate (a) and a pulse-plated zone plate (b). The diffraction efficiency profile is more uniform for the pulse-plated zone plate (d) than for the DC-plated one (c).

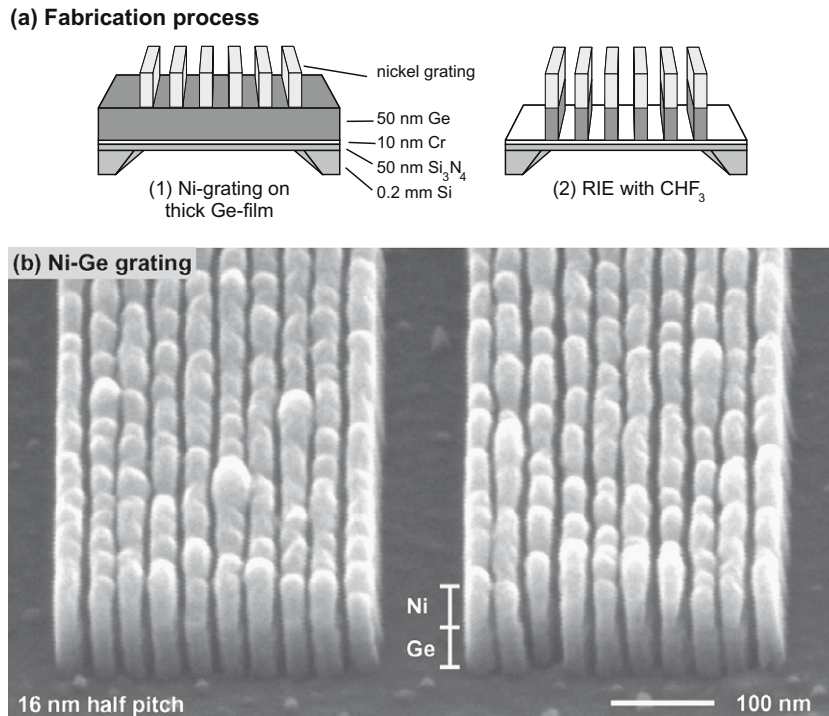


Fig. 3. (a) The fabrication process for Ni-Ge zone plate. A nickel zone plate is first fabricated on a germanium film and afterwards used as hard mask for dry etching into the germanium layer. (b) 16 nm gratings composed of ~50 nm Ni (top) and ~50 nm Ge (bottom).

Fig. 3a describes the fabrication process, which is very similar to that described in Section 2.1 and therefore only the steps and parameters that differ are discussed below. The silicon nitride substrates were coated with a 10 nm Cr etch stop and a 50 nm Ge film. The trilayer resist in this case consisted of a 55 nm thick plating mold material, PI-2610 (HD Microsystems), a 5 nm SiO₂ hard mask, and a 20 nm thick electron beam resist, ZEP 7000 (Zeon Chem., L.P.). The SiO₂ was sputter deposited (AJA Orion, 10⁻⁸ base pressure) and the PI-2610 was spincoated and baked for 120 min at

350 °C. The electron beam resist was patterned with a dose of ~300 μA/cm². This dose is necessary as the sensitivity of the resist is decreased when developing at low temperatures. The samples were developed in hexyl acetate for 30 s at -50 °C. The pattern transfer to the SiO₂ hardmask was performed by RIE with CHF₃ using 10 sccm gas flow, 10 mTorr pressure, 25 W sample RF power, and an etch time of 40 s. DC plating was used as pulse plating has not yet been implemented into this process. After the electroplating, the mold was removed by RIE. At this step, the nickel grating

was completed and used as a hardmask for CHF_3 dry etching into the underlying germanium. The etch parameters were: 10 min etch time, 10 sccm CHF_3 gas flow, 3 mTorr pressure, and 100 W sample RF power.

In Fig. 3b 16 nm half-pitch gratings with a total height of 100 nm are shown. They consist of 50 nm nickel (top) and 50 nm germanium (bottom). For a zone plate, this would result in a theoretical efficiency of 7.13% which should be compared with 3.22% for a 50 nm thick nickel zone plate. This result demonstrates that the nickel–germanium process is applicable for the fabrication of zone plates with twice the diffraction efficiency and with dr_N down to at least 16 nm.

4. Summary

We have demonstrated two approaches to improve the diffraction efficiency of high-resolution soft X-ray nickel zone plates. Pulse electroplating was applied to improve the mass distribution compared to DC plating, resulting in an increase of 20% in total diffraction efficiency. Nickel–germanium structuring was combined with cold development to yield a process for high diffraction efficiency and high resolution. 16 nm half-pitch gratings composed of 50 nm nickel on top of 50 nm germanium were fabricated, paving the way to zone plates with $\text{dr}_N = 16$ nm and with twice the diffraction efficiency of a regular nickel zone plate. In the future we will combine pulse plating and germanium-etching to further optimize the diffraction efficiency. Together with cold development, this will be used to fabricate high-resolution zone plates with improved diffraction efficiency.

Acknowledgements

We gratefully acknowledge the financial support of the Swedish Science Research Council, the Swedish Foundation for Strategic Research, the Wallenberg Foundation, and the Göran Gustafsson Foundation.

References

- [1] S. Aoki, Y. Kagoshima, Y. Suzuki (Eds.), in: Proceedings of the 8th International Conference on X-ray Microscopy, Inst. Pure Appl. Phys. (Jpn) Conf. Series 7 (2006).
- [2] D. Sayre, J. Kirz, R. Federer, D.M. Kim, E. Spiller, *Ultramicroscopy* 2 (1977) 337.
- [3] D.T. Attwood, *Soft X-Rays and Extreme Ultraviolet Radiation*, Cambridge University Press, Cambridge, 1999. pp. 337–394.
- [4] M. Lindblom, J. Reinspach, O.v. Hofsten, M. Bertilson, H.M. Hertz, A. Holmberg, *J. Vac. Sci. Technol.*, B 27 (2009) L1.
- [5] S.J. Spector, C.J. Jacobsen, D.M. Tennant, *J. Vac. Sci. Technol.*, B 15 (1997) 2872.
- [6] M. Peuker, *Appl. Phys. Lett.* 78 (2001) 2208.
- [7] J. Kirz, *J. Opt. Soc. Am.* 64 (1974) 301.
- [8] P.A.C. Takman, H. Stollberg, G.A. Johansson, A. Holmberg, M. Lindblom, H.M. Hertz, *J. Microsc.* 226 (2007) 175.
- [9] M. Lindblom, H.M. Hertz, A. Holmberg, *J. Vac. Sci. Technol.*, B 24 (2006) 2848.
- [10] M. Lindblom, J. Reinspach, O.v. Hofsten, M. Bertilson, H.M. Hertz, A. Holmberg, *J. Vac. Sci. Technol.*, B 27 (2009) L5.
- [11] O. Dossenbach, in: J.-C. Puipe, F. Leaman (Eds.), *Theory and Practice of Pulse Plating*, American Electroplaters and Surface Finishers Society, Orlando, FL, 1986, pp. 73–92.
- [12] A. Holmberg, S. Rehbein, H.M. Hertz, *Microelectron. Eng.* 73–74 (2004) 639.
- [13] M. Bertilson, P.A.C. Takman, U. Vogt, A. Holmberg, H.M. Hertz, *Rev. Sci. Instrum.* 78 (2007) 026103-3.
- [14] J. Reinspach, M. Lindblom, O.v. Hofsten, M. Bertilson, H.M. Hertz, A. Holmberg, *J. Vac. Sci. Technol.*, B, in press.